Lung Cancer 136 (2019) 57–64

Contents lists available at ScienceDirect

Lung Cancer

journal homepage: www.elsevier.com/locate/lungcan

Correlation between maximum standardized uptake values on FDG-PET and microenvironmental factors in patients with clinical stage IA radiologic pure-solid lung adenocarcinoma

Tomohiro Ichikawa[a,b,c], Keiju Aokage[b], Tomohiro Miyoshi[b], Kenta Tane[b], Kenji Suzuki[c], Hideki Makinoshima[d], Masahiro Tsuboi[b], Genichiro Ishii[a,*]

[a] Division of Pathology, Exploratory Oncology Research & Clinical Trial Center, National Cancer Center, Kashiwa, Chiba, Japan
[b] Department of Thoracic Surgery, National Cancer Center Hospital, Kashiwa, Chiba, Japan
[c] Departments of General Thoracic Surgery, Juntendo University School of Medicine, Tokyo, Japan
[d] Tsuruoka Metabolomics Laboratory, National Cancer Center, Tsuruoka, Japan

ARTICLE INFO

Keywords:
Lung cancer
18F-FDG PET
Tumor microenvironment

ABSTRACT

Objectives: The purpose of this study was to investigate whether fluorodeoxyglucose (FDG) accumulation is associated with the expression of microenvironmental factors in radiological pure-solid lung adenocarcinoma.
Methods: We selected 50 cases involving patients with clinical stage IA radiological pure-solid lung adenocarcinoma who were examined with 18 F-FDG positron emission tomography (18 F-FDG PET) prior to surgery and whose FDG–PET maximal standardized uptake values (SUVmax) were calculated. Tumor specimens were analyzed by immunohistochemistry (IHC) for phosphorylated AKT (pAKT), glucose transporter type 1 (GLUT-1), carbonic anhydrase IX (CA IX), podoplanin-positive cancer associated fibroblasts (PDPN + CAFs), and CD204-positive tumor-associated macrophages (CD204+ TAMs). We compared the clinicopathological characteristics and the immunophenotypes between two groups with high and low SUVmax.
Results: A multivariate analysis revealed that SUVmax was an independently significant prognostic factor ($P = .03$). The 5-year overall survival (OS) and recurrence free survival (RFS) rates of the SUV max high and low groups were 68.0% versus 100% (($P = .002$; OS) 54.3% versus 90.8% ($P < .001$; RFS)), respectively. Vascular invasion, pleural invasion, and the prevalence of solid predominant subtype tumors were more frequent in the SUVmax high group. Additionally, the expression levels of GLUT-1 and pAKT in cancer cells were significantly higher in this group ($P < .001$, and $P < .001$ respectively). Furthermore, the numbers of the tumor-promoting stromal cells, i.e., PDPN + CAFs and CD204+ TAMs, were also significantly higher in the SUVmax high group ($P = .001$, and $P < .001$ respectively).
Conclusion: Our results indicated that a close association exists between the SUVmax and expressions of not only metabolism associated markers in cancer cells but also of tumor promoting markers in stromal cells among patients with clinical stage IA adenocarcinoma with radiologically pure-solid nodules.

1. Introduction

The maximum standardized uptake value (SUVmax) on positron emission tomography with [18F] fluorodeoxyglucose (18F-FDG PET) is a promising modality for predicting the prognosis and invasiveness of lung adenocarcinoma [1,2]. Especially in cases where tumors had pure-solid appearances on thin-section CT scans, the SUVmax on PET reflected the levels of tumor invasiveness and had a great effect on the prognoses [3]. The SUVmax has been shown to be associated with histology in lung cancer. The low SUVmax levels correlated well with lepidic predominance among clinical stage IA radiologic pure-solid lung adenocarcinoma patients [4]. On the other hand, Kadota et al. reported that, among patients with the same histological grade of stage I lung adenocarcinoma based on the International Association for the Study of Lung Cancer/American Thoracic Society/European Respiratory Society (IASLC/ATS/ERS) classification, patients with high SUVmax were at a higher risk of recurrence than those with low SUVmax [5]. Thus, the SUVmax levels provide information on the biological behaviors among

* Corresponding author at: Division of Pathology, Exploratory Oncology Research and Clinical Trial Center, National Cancer Center, 6-5-1, Kashiwanoha, Kashiwa, Chiba 277-8577, Japan.
E-mail address: gishi@east.ncc.go.jp (G. Ishii).

https://doi.org/10.1016/j.lungcan.2019.08.003
Received 3 April 2019; Received in revised form 26 July 2019; Accepted 2 August 2019
0169-5002/ © 2019 Elsevier B.V. All rights reserved.

tumors beyond their histological differences.

The relationship between the cancer cell physiology and quantitative FDG uptake on PET has been investigated. Compared to normal cells, cancer cells often have higher rates of glucose metabolism to support their rapid proliferation. Furthermore, under low oxygen supply, highly proliferative tumor cells switch their glucose metabolism pathway away from mitochondrial oxidative phosphorylation to generate lactate. 18 F-FDG uptake is seemingly regulated by the glucose metabolism based on the data demonstrating that the overexpression of glucose transporter type 1 (GLUT-1) is significantly correlated with this uptake in human neoplasms [6]. Several studies have shown that higher SUVmax on 18 F-FDG PET is associated with elevated tumor levels of GLUT-1 and the results of the former study revealed that the amount of 18 F-FDG uptake was closely correlated withPI3K/Akt/mTOR signaling pathway [7,8].

Cancer tissue comprises not only of cancer cells but also of different kinds of stromal cells, which are commonly found in association with cancer cells [9]. While epithelium cells have been investigated for a long time, it is not yet well known how stromal cells influence cancer metabolism. A recent study has proposed a new idea called the “reverse Warburg effect.” According to this theory, the epithelial cancer cells instruct the normal stroma to transform into cancer-associated fibroblasts (CAFs); following this, aerobic glycolysis is induced in the CAFs, which then produce energy-rich metabolites, such as lactate and pyruvate, that are secreted and used by epithelial cells to generate adenosine tri-phosphate (ATP) [10]. Lisanti et al. showed that CAFs increased their glucose uptake when the cancer cells and fibroblasts co-cultured, and they suggested that PET imaging of human tumors may be specifically detecting the tumor stroma rather than epithelial cancer cells [11]. In addition to fibroblasts, the tumor microenvironment consists of various cell types, including tumor infiltrating lymphocytes (TILs) and tumor-associated macrophages (TAMs) [12,13]. A former study reported that FDG was actively entrapped in not only neoplastic tissue but also tumor-related activated immune cells, such as the TILs and TAMs [14,15].

Based on former studies, we speculated that FDG uptake might be associated with stromal cell markers. We have previously reported that podoplanin-positive CAFs (PDPN + CAFs) as well as CD204-positive TAMs (CD204 + TAMs) have tumor-promoting functions in lung cancer [16,17]. In this study, we tried to examine the correlation between SUVmax on ^{18}F-FDG PET and the expression of tumor promoting stromal markers.

To this end, we only focused on radiologically pure-solid lung adenocarcinoma to keep our subjects homogeneous.

2. Material and methods

2.1. Patients

To select the study participants, we retrospectively searched through our institute’s database for patients who had undergone complete tumor resections by lobectomy, and complete hilar and mediastinal lymph node dissection for clinical stage IA lung adenocarcinoma between January 2006 and December 2012. Among 772 patients, 116 patients underwent a preoperative evaluation via 18 F-FDG-PET. Patients who had previously received lung surgeries or preoperative therapies, including chemotherapy and radiotherapy, were excluded from this study. Any clinical stage IA lung adenocarcinoma case involving a ground-glass opacity (GGO) component was excluded from the study. The remaining 50 patients were retrospectively evaluated in this study. This study was approved by the institutional review board of the National Cancer Center (approval numbers 2018-021). Each patient was informed that his or her clinical data could be used for various studies and comprehensive informed consent was obtained on that basis.

Table 1
Univariate and multivariate analysis on factors influencing disease free survival.

Variables	Univariate Analysis		Multivariate Analysis	
	HR (95% CI)	*P* Value	HR (95% CI)	*P* Value
Age	1.02 (0.97–1.09)	0.42		
Sex (male)	0.97 (0.33–2.76)	0.95		
Smoking Index	1.00 (0.99–1.00)	0.16		
Maximum tumor size (cm)	1.77 (0.66–4.76)	0.25		
Air-brinchogram (absent)	0.57 (00.18–1.83)	0.34		
SUVmax	1.25 (1.10–1.43)	< 0.01	1.18 (1.02–1.38)	0.03
CEA (ng/mL)	1.09 (1.04–1.14)	< 0.01	1.06 (1.01–1.11)	0.03

2.2. Radiologic evaluations on thin-section computed tomography (CT) scans

For all patients, thin-section CT scans were performed to assess the clinical staging. The X-vigor CT system (Toshiba Medical Systems, Tokyo, Japan) was used to perform the CT scans, and the CT images were evaluated on a monitor display with a window level of 600 Hounsfield units and a window width of 1800 Hounsfield units. Tumor sizes were determined preoperatively based on thin-section CT scans with a 1–2 mm collimation in the lung window. In the current study, a radiologic pure-solid tumor was defined as one that did not include a GGO component, which in turn was defined as an area of increased hazy density that did not obscure the underlying vascular structure within the area being scanned.

2.3. FDG-PET/CT

As detailed in a previous study [18], the FDG-PET/CT examinations were performed with a Discovery LS8 (GE Healthcare, Milwaukee, WI, USA). The axial field of view (FOV) was 15.7 cm, and spatial resolution, 6.2 mm of full-width-half-maximum. The PET scans were performed using a two-dimensional acquisition mode from the thigh to the skull base with seven bed positions. Each bed position included 1 min of transmission scanning and 5 min of emission scanning.

The CT component of both the PET/CT scanners was a 16-row multidetector CT scanner; CT images were acquired with a tube voltage of 140 kV, and the tube current was automatically set using the auto-exposure control function to limit the number of standard deviations caused by noise to 10. The attenuation corrections of the PET images were performed using the data from the CT images. The PET images were reconstructed via an iterative reconstruction with an ordered-subset expectation maximization algorithm (two iterations, 14 subsets) and were reformatted into transverse, coronal, and sagittal views. All the PET and CT images were interpreted by experienced radiologists.

2.4. Histological evaluation

All specimens were fixed with 10% formalin or methanol via infusion through the bronchial tree and then embedded in paraffin. The tumors were sliced at approximately 5 mm intervals, and serial 4 μm sections were stained with hematoxylin-eosin (H-E). The Alcian blue-periodic acid Schiff and Verhoeff-Van Gieson (VVG) staining methods were performed to visualize cytoplasmic mucin production and elastic fibers, respectively. All the slides, each mounted with a section representing the maximum surface area of the tumor from each case, were coded, masked for identifiable information, and reviewed by two pathologists (T.I. and G.I.). Vascular and pleural invasions were determined by VVG staining. Lymphatic permeation was determined via

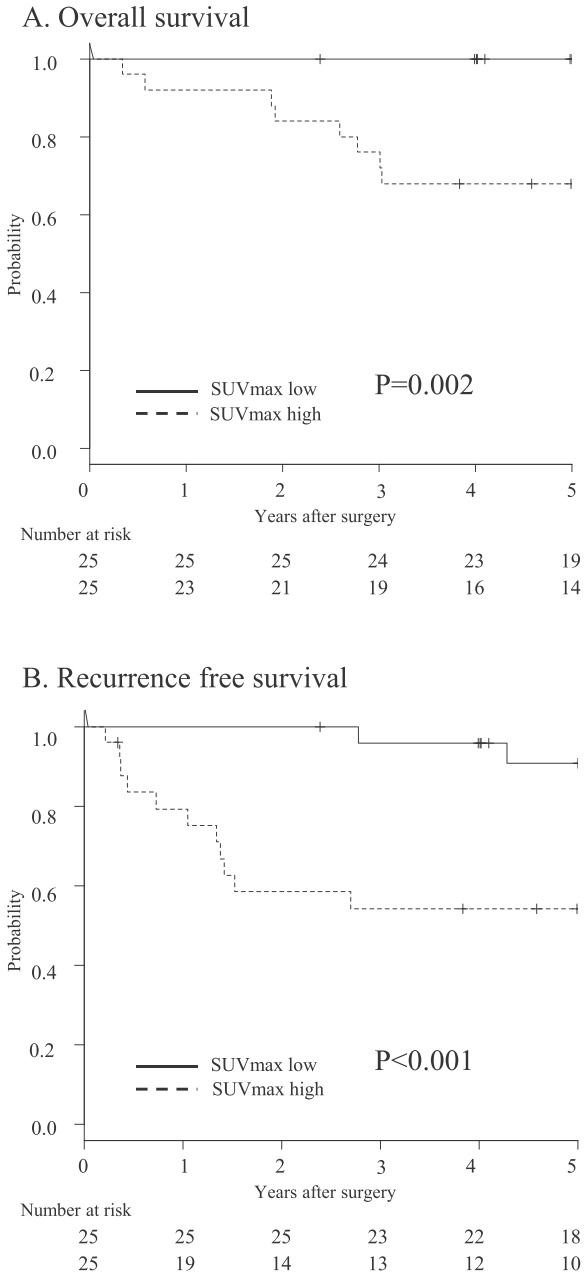

Fig. 1. Overall survival and recurrence free survival rates of the SUVmax high and low groups. Kaplan-Meier curves showing overall survival (A) and recurrence-free survival (B) of patients according to the 18F-FDG uptake.

sections stained with H-E. Histological diagnoses were based on the 4th revised World Health Organization (WHO) histologic classifications. The specimens were classified as lepidic, acinar, papillary, solid, or micropapillary according to the 4th edition of the WHO Classification of Tumors of the Lung, Pleura, Thymus and Heart; the percentages of each subtype were shown in the histology reports, with the subtype occupying the largest area considered as the predominant subtype. The invasive component was clearly defined according to the IASLC/ATS/ERS consensus report. All the tumors were staged pathologically using the 8th edition of the TNM classification of lung cancer published by the IASLC.

2.5. Immunohistochemical staining

Immunohistochemical staining was performed according to a previously reported method [19]. For the markers of carcinoma cells, pAKT (1:50, Cell Signaling Technology Inc.), GLUT-1 (1:500, SPRING Bioscience), and carbonic anhydrase IX (CA IX) (1:500, Proteintech) were evaluated. For stromal cell markers, CD204 (1:400, SRA-E5, Trans Genic, Japan) was used as a tumor associated M2 macrophage marker, and PDPN (1:50, D2-40, Acris Antibodies) was used as a tumor promoting CAF marker.

Table 2
Clinicopathological differences between SUV max high and low.

Variables	SUV max high (SUVmax ≥ 5.4) (n = 25)	SUV max low (SUVmax < 5.4) (n = 25)	p-value
Age (range)	70 (76-93)	69 (76-81)	0.72
Gender			
Male	13 (52%)	12 (48%)	0.99
Female	12 (48%)	13 (52%)	
Smoking status			
Never smoker	10 (40%)	14 (56%)	0.40
Ever smoker	15 (60%)	11 (44%)	
CEA (ng/ml)			
≤ 5.0	12 (48%)	21 (84%)	0.02
> 5.0	13 (52%)	4 (16%)	
Radiological maximum tumor size	2.4 cm (1.2-2.8)	1.9 cm (1.1-3.0)	0.06
Clinical T stage			
cT1b	8 (32%)	14 (56%)	0.15
cT1c	17 (68%)	11 (44%)	
Air-bronchogram	8 (32%)	12 (48%)	0.38
pN status			
N0	19 (76%)	24 (96%)	0.09
N1-N2	6 (24%)	1 (4%)	
Lymphatic permeation			
Absent	18 (72%)	22 (88%)	0.29
Present	7 (28%)	3 (12%)	
Vascular invasion			
Absent	7 (28%)	21 (84%)	< 0.01
Present	18 (72%)	4 (16%)	
Pleural invasion			
Absent	13 (52%)	22 (88%)	0.01
Present	12 (48%)	3 (12%)	
Pathological maximum tumor size	2.5 cm (1.0-3.2)	1.8 cm (1.0-3.6)	0.01
Pathological invasive size	2.3 cm (1.0-3.2)	1.5 cm (0.2-2.5)	< 0.01
Pathological stage			< 0.01[a]
IA1	1 (4%)	7 (28%)	
IA2	1 (4%)	12 (48%)	
IA3	9 (36%)	2 (8%)	
IB	7 (28%)	3 (12%)	
IIA	0	0	
IIB	1 (4%)	1 (4%)	
IIIA	6 (24%)	0	
Predominant subtype			0.01
lepidic	0	2 (8%)	
acinar or papillary	15 (60%)	21 (82%)	
solid	10 (40%)	(8%)	

2.6. Calculation of immunohistochemical scores

Immunostaining scores were the products of the staining-intensity scores and percentages of positively stained cells, except for CD204+ cells. The staining intensity scores were as follows: 0 (negative; total absence of staining), 1+ (weak staining), and 2+ (strong staining); these were multiplied by the percentages of immunohistochemically stained tumor cells per section (0–100%), resulting in scores ranging from 0 to 200. The numbers of CD204+ TAMs were counted under a light microscope using high power fields (HPF, 400 x :0.0625 mm^2/field) because TAMs are countable. The averages of the number of positive cells in 3 HPFs were recorded as the scores of CD204+ TAMs. All the immunohistochemical slides were evaluated by two independent pathologists (T.I. and G.I.). Both were unaware of the clinical and pathological information.

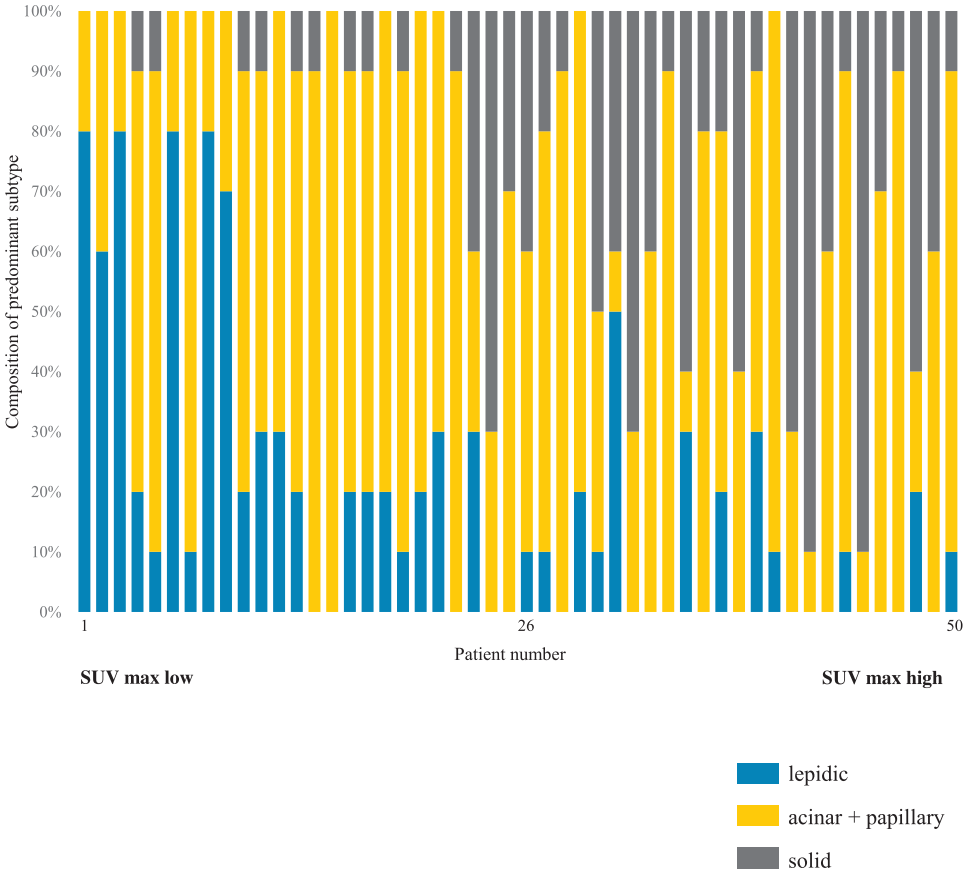

Fig. 2. Proportion of histological subtypes in each of the cases. Each of the cases were arranged according to the SUVmax. Blue: lepidic predominant component, yellow: acinar and papillary predominant components, and black: solid predominant component (For interpretation of the references to colour in this figure legend, the reader is referred to the web version of this article).

2.7. Statistical analysis

The cumulative overall survival and recurrence free survival rates were estimated by the Kaplan-Meier method and compared using the log-rank test. The date of surgical resection was set as the starting point and the date of death or last date of follow-up as the end point. Univariable and multivariable Cox regression analyses were performed to assess the impact of the subgroups on overall survival for only clinical and radiological factors. Unpaired *t*-test or chi-square test was used to compare clinicopathological factors between two variables. Mann- Whitney U test was used for immunostaining scores. For rank correlation, we used Spearman' correlation coefficient test. All the statistical calculations were performed by JMP software (version 10.0, SAS Institute, Cary, NC). Statistical analysis was considered significant when the probability value was less than 0.05.

3. Results

3.1. Association between clinical factors and recurrence

Fifty patients with a median age of 69 years (range, 38–93), who had clinical stage IA lung adenocarcinoma with lobectomies and lymph node dissections were included in this study. Twenty-four (48%) were male, and 26 (52%) were smokers. The median SUVmax of all the primary tumors was 5.3 (range, 0–16.9). The average radiological maximum tumor diameter was 2.1 cm. The numbers of patients at clinical stage IA1, IA2, IA3 were 0, 22 (44%), and 28 (56%), respectively.

Firstly, univariable and multivariable Cox regression analyses were performed to assess whether SUVmax was the prognostic factor in this cohort or not. The univariate analysis on the data associated with RFS demonstrated that SUVmax ($P < .01$) and the serum carcinoembryonic antigen (CEA) levels ($P < .01$) were significantly associated with poor prognoses. The multivariate analysis revealed that SUVmax (hazard ratio [HR], 1.18; 95% confidence interval [CI], 1.02–1.38; $P = 0.03$) as well as CEA levels (HR, 1.06; 95% CI, 1.01–1.11; $P = 0.003$) were independent prognostic factors (Table 1).

3.2. Prognosis of patients according to 18 F-FDG uptake on PET

Furthermore, we divided the clinical stage IA pure-solid lung adenocarcinomas into two categories based on the SUVmax. We considered patients with "SUVmax > median" as the "SUVmax high group" (n = 25). The same was done for patients with a "SUVmax < median," who were allocated to the "SUVmax low group" (n = 25). Supplemental Fig. 1 shows representative thin-section CTs and PET-CTs in patients with low and high 18 F-FDG uptakes. The median follow-up time in censored cases was 5.2 years. The five-year OS (Fig. 1A) and five-year RFS (Fig. 1B) rates were significantly higher in patients with low 18 F-FDG uptakes than those in patents with high 18 F-FDG uptakes (100% vs. 68.0%, $P = 0.002$; 90.8% vs. 48.9 and 54.3%, $P < 0.001$, respectively)

3.3. Clinicopathological differences between the SUVmax high and low groups

Table 2 presents the results of an evaluation of the relationships between the data of the SUVmax high and low groups. Clinically, patients with low SUVmax showed significant serum CEA levels of 5 ng/mL or less ($P = 0.02$). The radiological maximum tumor sizes and the number of clinical T1c patients were considerably higher in the SUVmax high group though the difference was not statistically significant ($P = 0.06$, and 0.15 respectively). Pathologically, vascular and pleural invasions were more common in patients with high SUVmax. Median total and invasive tumor sizes were 2.5 and 2.3 cm in the SUVmax high group (range, 1.0–3.2 cm, respectively). Compared to the

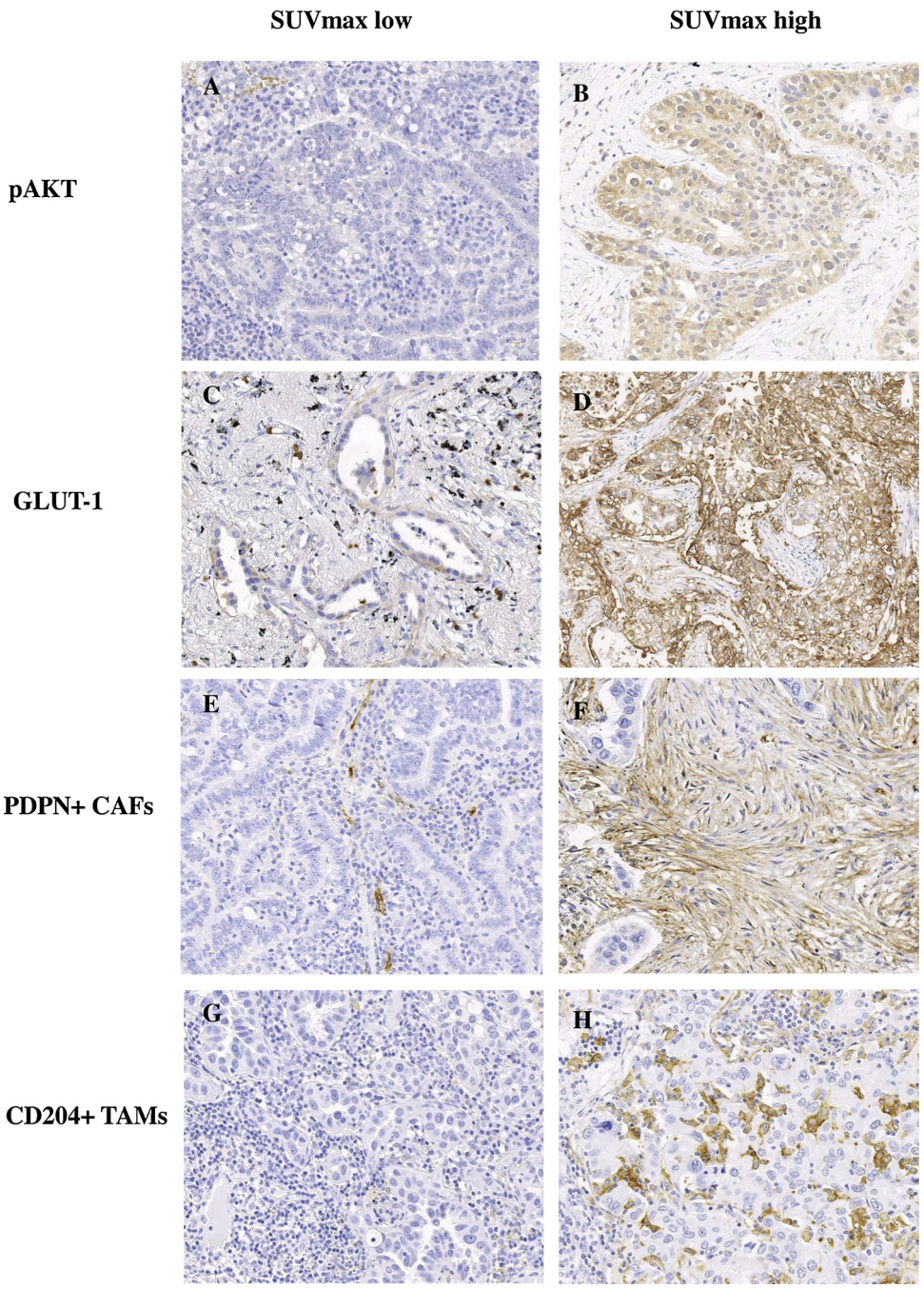

Fig. 3. Immunohistochemical staining for phosphorylated AKT (pAKT), glucose transporter type 1 (GLUT-1), podoplanin-positive cancer associated fibroblasts (PDPN + CAFs), and CD204 positive tumor associated macrophages (TAMs) in specimens from the SUVmax high and low groups, respectively.

SUVmax low group, both total and invasive tumor sizes were significantly large in this group. (P = 0. 01, and < 0.01 respectively) The number of patients with pathological stage IB or higher was 14 (56%) in the SUVmax high group and 4 (16%) in the SUVmax low group (P < 0.01). A histological subtype evaluation revealed that solid predominant lung adenocarcinoma was more frequent in the patients with high SUVmax (10 of 25 (40%)) than in those with low SUVmax (2 of 25 (8%)) (P = 0. 02). Fig. 2 presents the proportion of the histological subtypes in each of the cases, which were arranged in the order of the levels of SUVmax from left to right. A large proportion of tumors from the cases with lower SUVmax were comprised of the lepidic predominant subtype. On the other hand, the solid predominant subtype accounts for the largest proportion among the cases with higher SUVmax.

3.4. Correlations between SUVmax and immunochemical staining scores

GLUT-1 (Fig. 3A and B) and pAKT (Fig. 3C and D) expressions within tumor cells were significantly higher in patients from the SUVmax high group compared with in patients from the SUVmax low group (P < 0.01). The staining scores (expressed as means ± SD) of PDPN + CAFs (Fig. 3E and F) in the SUVmax high and low groups were 16.4 ± 19.8 and 4.8 ± 10.5, respectively, and the corresponding scores for CD204+ TAMs (Fig. 3G and H) were 37.9 ± 34.2 and 14.8 ± 15.9, respectively. These scores in the SUVmax high group were significantly higher than those in the SUVmax low group (PDPN + CAFs: P = 0.01, CD204+ TAMs: P < 0.01) (Fig. 4 and Supplemental Table 1). We found a statistically significant correlation between SUVmax with the expressions of PDPN + CAFs (rho = 0.51;

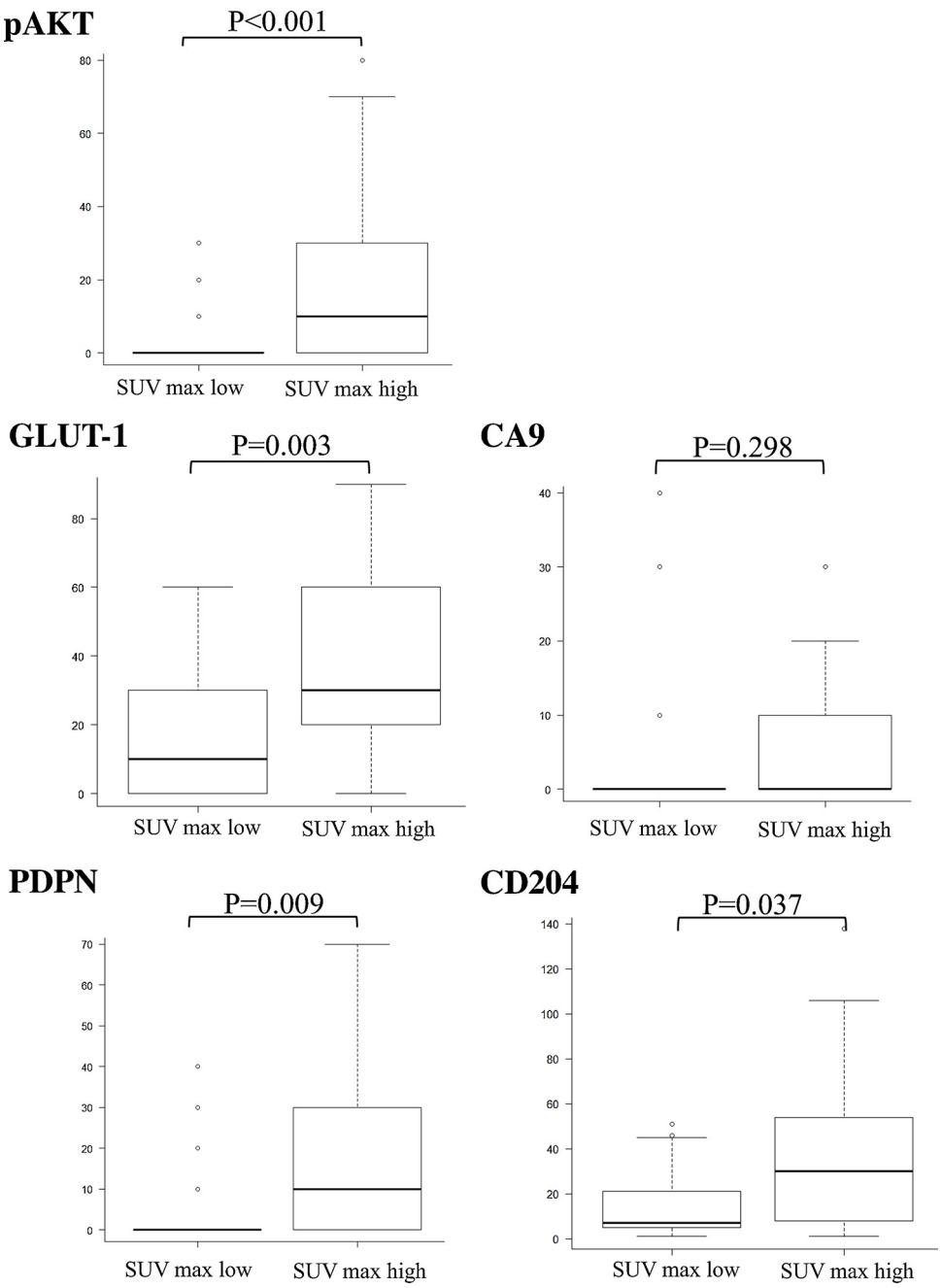

Fig. 4. Immunohistochemical scores of phosphorylated AKT (pAKT), glucose transporter type 1 (GLUT-1), carbonic anhydrase IX (CA 9), podoplanin-positive cancer associated fibroblasts (PDPN + CAFs), and CD204 positive tumor associated macrophages (TAMs) according to the SUVmax.

P < 0.001) and CD204 + TAMs (rho = 0.43; P = 0.002). Also, GLUT-1 and pAKT expressions in cancer cells strongly correlated with SUVmax (rho = 0.56; P < 0.001, and rho = 0.33; P = 0.02). (Supplemental Fig. 2)

4. Discussion

Cancer cells frequently have predominantly glycolytic metabolisms that are required for the growth of tumors as outlined by the "Warburg effect." 18 F-FDG uptake on PET is seemingly regulated by glucose metabolism, and previous studies have demonstrated the correlation between tumor 18 F-FDG uptake and GLUT-1 expression in human neoplasms. However, there are no studies on the correlation of 18 F-FDG uptake with the number of stroma cells of the tumor microenvironment. In this study, we examined the relationship between the microenvironmental factors and FDG uptake on PET, and we found that the numbers of tumor promoting stromal cells such as the PDPN + CAFs and CD204 + TAMs were higher in patients with high SUVmax on 18 F-FDG PETs. To our knowledge, this is the first study to investigate the correlation between the 18 F-FDG uptake and the numbers of tumor promoting stromal cells.

In this study, GLUT-1 and pAKT expressions within tumor cells were significantly higher in patients from the SUVmax high group. These results agree with those of previous studies [7,8]. In addition, solid predominant lung adenocarcinoma was more frequent in the patients with high SUVmax (P = 0. 02). Former studies have reported on a positive association between the SUVmax and histologic grade. Hattori et al. revealed that the SUVmax was an independently significant variable of lepidic predominant adenocarcinoma [4]. Kadota et al. studied the association between the SUVmax and histologic grade based

on the IASLC/ATS/ERS classification. Solid predominant invasive adenocarcinoma had the highest SUVmax, followed by acinar, papillary, and lepidic predominant adenocarcinomas [5]. Kaira et al. demonstrated that the glucose metabolism in cancer tissues measured on 18 F-FDG PET/CT is a significant biomarker of the aggressiveness of tumors [20]. The results of these studies are consistent with our results.

Hypoxia can increase GLUT-1 levels and glucose uptake, and a relation between expression of glucose transporters and FDG uptake has been reported [21,22]. Therefore, the degree of tumor FDG uptake may reflect the level of hypoxia. In this study, we investigated the impact of tumor hypoxia on the uptake of FDG, as assessed by the expression of the CAIX, and there was no correlation between FDG uptake and CAIX. This result is consistent with previous studies [23,24]. According to these studies, FDG uptake does not seem to reflect the level of hypoxia.

We have previously shown that solid predominant adenocarcinoma displayed a higher number of tumor-promoting stromal cells, PDPN + CAFs and CD204+ TAMs, than the other subtypes [25]. Thus, the higher number of tumor-promoting stromal cells in the SUVmax high group may be due to the solid predominant histological subtype. We validated the association between the SUVmax and expressions of tumor-promoting stromal markers in a more uniform cohort excluding the solid predominant cases (predominant acinar or papillary subtype, n = 36), (Supplemental Fig. 3). The expressions of PDPN + CAFs (rho = 0.45; $P < 0.001$) and CD204+ TAMs (rho = 0.43; P = 0.002) significantly correlated with the SUVmax. Thus, an abundance of tumor promoting stromal cells (PDPN + CAFs and CD204+ TAMs) might lead to higher SUVmax regardless of the histological subtype.

Recent studies showed that the FDG uptake might also be increased in non-cancerous stromal cells in tumors [26,27]. However, it is not clear whether the cancer cells that were instructed by the tumor promoting stromal cells take up FDGs or whether the tumor promoting stromal cells directly integrate FDGs. We could not confirm the answer to this question in this study. Thus, our next study will aim to investigate the relationship between stromal cells and glucose metabolism.

In the tumor microenvironment, large amount of lactate is released as a result of glycolysis. Then, lactic acid has been shown to shape the functional phenotype of the immune cells [28]. Colegio et al. showed that lactate induced the expression of ARG-1 and VEGF in TAMs, and polarized their activation toward to M2 state [29]. These reports support our result that SUVmax correlate with the number of CD 204 TAMs.

According to the current study, the prognoses of radiologically pure-solid adenocarcinoma were different based on the SUVmax levels (Fig. 1 and Table 1). Moreover, the SUVmax levels correlated well with the pathological invasiveness of the cancer and the histologic subtypes based on the IASLC/ATS/ETS classification (Fig. 2 and Table 2) Our findings are compatible with former studies. A recent review by Nair et al. examined the effects of FDG uptake on the survival rates of patients with early-stage non-small-cell lung carcinoma (NSCLC), and they found substantial evidence that the degree of FDG uptake in the primary tumor is associated with prognoses in patients with early-stage NSCLC [2]. Hattori et al. reported that SUVmax levels were the significant clinical factors that were predictive of the pathological invasive status—pleural invasion, lymphatic invasion, vessel invasion, and nodal metastasis—of resected clinical stage IA radiologically pure-solid lung cancer [4,30].

There were several limitations in the current study. This was a retrospective study carried out at a single institution on an ethnically homogenous population. The total number of cases was relatively small. However, this is the first study to investigate the correlation between the 18 F-FDG uptake and the number of tumor-promoting stromal cells in lung adenocarcinoma. This study suggests that the SUVmax might be used as a noninvasive tool to assess the tumor microenvironment including the frequency of tumor promoting stromal cells.

Ethical approval

All procedures performed in studies involving human participants were in accordance with the ethical standards of the institutional and national research committee and with the 1964 Helsinki declaration and its later amendments or comparable ethical standards.

Informed consent

Comprehensive informed consent was obtained in the study. IRB approval number of this study is 2018-21.

Transparency document

The Transparency document associated with this article can be found in the online version.

Declaration of Competing Interest

The authors have no conflict of interests to disclose.

Acknowledgments

This work was supported in part by the Foundation for the JSPS KAKENHI (16H05311).

Appendix A. Supplementary data

Supplementary material related to this article can be found, in the online version, at doi:https://doi.org/10.1016/j.lungcan.2019.08.003.

References

[1] J. Vansteenkiste, B.M. Fischer, C. Dooms, et al., Positron-emission tomography in prognostic and therapeutic assessment of lung cancer: systematic review, Lancet Oncol. 5 (September (9)) (2004) 531–540.
[2] V.S. Nair, P.G. Barnett, et al., Ananth LPET scan 18F-fluorodeoxyglucose uptake and prognosis in patients with resected clinical stage IA non-small cell lung cancer, Chest 137 (May (5)) (2010) 1150–1156.
[3] A. Hattori, T. Matsunaga, K. Suzuki, et al., Clinical significance of positron emission tomography in subcentimeter non-small cell lung Cancer, Ann. Thorac. Surg. 103 (May (5)) (2017) 1614–1620.
[4] A. Hattori, T. Matsunaga, K. Suzuki, et al., Indications for sublobar resection of clinical stage IA radiologic pure-solid lung adenocarcinoma, J. Thorac. Cardiovasc. Surg. 154 (2017) 1100–1108.
[5] K. Kadota, C. Colovos, P.S. Adusumilli, et al., FDG-PET SUVmax combined with IASLC/ATS/ERS histologic classification improves the prognostic stratification of patients with stage I lung adenocarcinoma, Ann. Surg. Oncol. 19 (2012) 3598–3605.
[6] K. Kaira, M. Endo, M. Abe, et al., Biologic correlation of 2-[18F]-fluoro-2-deoxy-d-glucose uptake on positron emission tomography in thymic epithelial tumors, J. Clin. Oncol. 28 (2010) 3746–3753.
[7] T. Furukawa, Y. Miyata, M. Okada, et al., Association between [18F]-fluoro-2-deoxyglucose uptake and expressions of hypoxia-induced factor 1α and glucose transporter 1 in non-small cell lung cancer, Jpn. J. Clin. Oncol. 45 (12) (2015) 1154–1161.
[8] T. Kamai, T. Mizuno, H. Abe, et al., Clinically significant association between the maximum standardized uptake value on 18F-FDG PET and expression of phosphorylated Akt and S6 kinase for prediction of the biological characteristics of renal cell cancer, BMC Cancer 15 (114) (2015).
[9] G. Ishii, A. Ochiai, S. Neri, Phenotypic and functional heterogeneity of cancer-associated fibroblast within the tumor microenvironment, Adv. Drug Deliv. Rev. 99 (April (Pt B)) (2016) 186–196.
[10] S. Pavlides, D. Whitaker-Menezes, R. Castello-Cros, et al., The reverse Warburg effect: aerobic glycolysis in cancer associated fibroblasts and the tumor stroma, Cell Cycle 8 (2009) 3984–4001.
[11] U.E. Martinez-Outschoorn, Z. Lin, M.P. Lisanti, et al., Cancer cells metabolically "fertilize" the tumor microenvironment with hydrogen peroxide, driving the Warburg effect Implications, Cell Cycle 15 (2010) 2504–2520.
[12] T.F. Gajewski, H. Schreiber, Y.X. Fu, Innate and adaptive immune cells in the tumor microenvironment, Nat. Immunol. 14 (2013) 1014–1022.
[13] D. Hanahan, L.M. Coussens, Accessories to the crime: functions of cells recruited to the tumor microenvironment, Cancer Cell 21 (2012) 309–322.
[14] E.M. Palsson-McDermott, L.A.J. O'Neill, The Warburg effect then and now: from cancer to inflammatory diseases, BioEssays 35 (2013) 965–973.

[15] R. Appelberg, D. Moreira, P. Barriera-Silva, et al., TheWarburg effect in mycobacterial granulomas is dependent on the recruitment and activation of macrophages by interferon-y, Immunology 145 (2015) 498–507.
[16] A. Hoshino, G. Ishii, T. Ito, et al., Podoplanin-positive fibroblasts enhance lung adenocarcinoma tumor formation: podoplanin in fibroblast functions for tumor progression, Cancer Res. 71 (July (14)) (2011) 4769–4779.
[17] R. Maeda, G. Ishii, S. Neri, et al., Circulating CD14 + CD204 + cells predict postoperative recurrence in non-small-cell lung cancer patients, J. Thorac. Oncol. 9 (February (2)) (2014) 179–188.
[18] S. Niho, H. Fujii, K. Murakami, et al., Detection of unsuspected distant metastases and/or regional nodes by FDG-PET in LD-SCLC scan in apparent limited-disease small-cell lung cancer, Lung Cancer 57 (2007) 328–333.
[19] M. Ito, G. Ishii, K. Nagai, et al., Prognostic impact of cancer-associated stromal cells in patients with stage I lung adenocarcinoma, Chest 142 (July (1)) (2012) 151–158.
[20] K. Kaira, Y. Koh, N. Yamamoto, et al., Biological significance of 18F-FDG uptake on PET in patients with non-small-cell lung cancer, Lung Cancer 83 (2014) 197–204.
[21] G.L. Semenza, Regulation of cancer cell metabolism by hypoxia-inducible factor 1rights, Semin. Cancer Biol. 19 (2009) 12–16.
[22] L.F. de Geus-Oei, J.H. van Krieken, R.P. Aliredjo, et al., Biological correlates of FDG uptake in non-small cell lung cancer, Lung Cancer 55 (2007) 79–87.
[23] A. van Baardwijk, C. Dooms, D. De Ruysscher, et al., The maximum uptake of (18)F-deoxyglucoseon positron emission tomography scan correlates with survival, hypoxiainducible factor-1alpha and GLUT-1 in non-small cell lung cancer, Eur. J. Cancer (Oxford, England : 1990) 43 (9) (2007) 1392–1398.
[24] Y.W. Koh, S.J. Lee, S.Y. Park, et al., Differential expression and prognostic significance of GLUT1according to histologic type of non-small-cell lung cancer and its association with volume-dependent parameters, Lung Cancer 104 (2017) 31–37.
[25] K. Goto, K. Saruwatari, G. Ishii, et al., Aggressive tumor microenvironment of solid predominant lung adenocarcinoma subtype harboring with epidermal growth factor receptor mutations, Lung Cancer 91 (2016) 7–14.
[26] C. Hensley, B. Faubert, R. DeBerardinis, et al., Metabolic heterogeneity in human lung tumors, Cell 164 (2016) 681–694.
[27] G. Zhang, J. Li, X. Wang, et al., The reverse Warburg effect and 18F-FDG uptake in non-small cell lung cancer A549 in mice: a pilot study, J. Nucl. Med. 56 (2015) 607–612.
[28] R.J. Arts, T.S. Plantinga, S. Tuit, et al., Transcriptional and metabolic reprogramming induce an inflammatory phenotype in non-medullary thyroid carcinoma-induced macrophages, Oncoimmunology 5 (2016) e1229725.
[29] O.R. Colegio, N.Q. Chu, A.L. Szabo, et al., Functional polarization of tumour-associated macrophages by tumour-derived lactic acid, Nature 513 (2014) 559e563.
[30] A. Hattori, M. Tatsuo, K. Suzuki, et al., Predictors of pathological non-invasive lung cancer with pure-solid appearance on computed tomography to identify possible candidates for sublobar resection, Surg. Today 46 (2016) 102–109.